AD-A060 151 AIR FORCE GEOPHYSICS LAB HANSCOM AFB MASS F/G 22/2
SPACECRAFT POTENTIAL CALCULATIONS -- A MODEL.(U)
MAY 78 H B GARRETT
UNCLASSIFIED AFGL-TR-78-0116 NL

| OF |
AD
A060151

END
DATE
FILMED
2-78
DDC

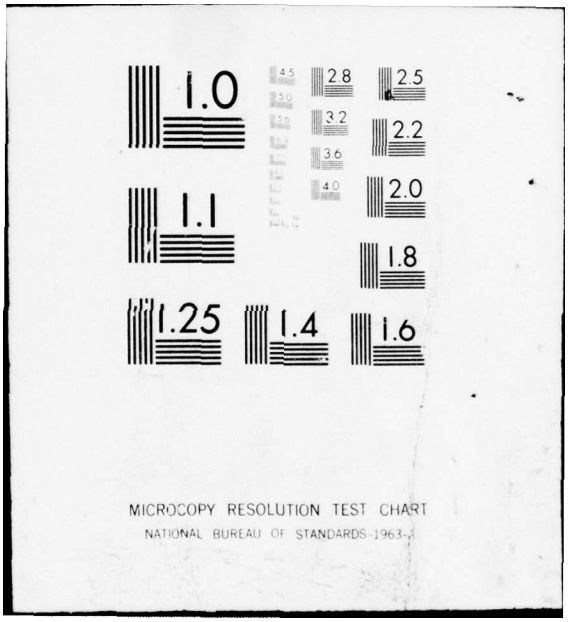
1.0
1.1
1.25
1.4
1.6
1.8
2.0
2.2
2.5
2.8
3.2
3.6
4.0
4.5
5.0
5.6
MICROCOPY RESOLUTION TEST CHART
NATIONAL BUREAU OF STANDARDS-1963-A

AFGL-TR-78-0116
AIR FORCE SURVEYS IN GEOPHYSICS, NO. 387

LEVEL II

Spacecraft Potential Calculations – A Model

HENRY B. GARRETT, Capt, USAF

5 May 1978

SPACE PHYSICS DIVISION PROJECT 7661
AIR FORCE GEOPHYSICS LABORATORY
HANSCOM AFB, MASSACHUSETTS 01731

AIR FORCE SYSTEMS COMMAND, USAF

This report has been reviewed by the ESD Information Office (OI) and is releasable to the National Technical Information Service (NTIS).

This technical report has been reviewed and
is approved for publication.

FOR THE COMMANDER

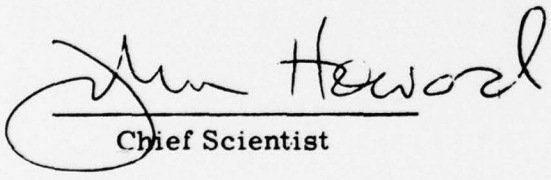

Chief Scientist

Qualified requestors may obtain additional copies from the Defense Documentation Center. All others should apply to the National Technical Information Service.

Unclassified

SECURITY CLASSIFICATION OF THIS PAGE (When Data Entered)

REPORT DOCUMENTATION PAGE	READ INSTRUCTIONS BEFORE COMPLETING FORM
1. REPORT NUMBER: AFGL-TR-78-0116	2. GOVT ACCESSION NO.: AFGL-AFSG-387	3. RECIPIENT'S CATALOG NUMBER:
4. TITLE (and Subtitle): SPACECRAFT POTENTIAL CALCULATIONS – A MODEL	5. TYPE OF REPORT & PERIOD COVERED: Scientific. Interim.
	6. PERFORMING ORG. REPORT NUMBER: AFSG No. 387
7. AUTHOR(s): Henry B. Garrett, CAPT, USAF	8. CONTRACT OR GRANT NUMBER(s):
9. PERFORMING ORGANIZATION NAME AND ADDRESS: Air Force Geophysics Laboratory (PHG) Hanscom AFB, Massachusetts 01731	10. PROGRAM ELEMENT, PROJECT, TASK AREA & WORK UNIT NUMBERS: 62101F 76610801
11. CONTROLLING OFFICE NAME AND ADDRESS: Air Force Geophysics Laboratory (PHG) Hanscom AFB, Massachusetts 01731	12. REPORT DATE: 5 May 1978
	13. NUMBER OF PAGES: 40
14. MONITORING AGENCY NAME & ADDRESS (if different from Controlling Office)	15. SECURITY CLASS. (of this report): Unclassified
	15a. DECLASSIFICATION/DOWNGRADING SCHEDULE

16. DISTRIBUTION STATEMENT (of this Report)

Approved for public release; distribution unlimited.

17. DISTRIBUTION STATEMENT (of the abstract entered in Block 20, if different from Report)

40 p.

18. SUPPLEMENTARY NOTES

Air Force surveys in geophysics,

19. KEY WORDS (Continue on reverse side if necessary and identify by block number)

Spacecraft charging
Plasma interactions
Satellite anomalies

20. ABSTRACT (Continue on reverse side if necessary and identify by block number)

A simple model for calculating the potential on a spacecraft by balancing the currents to and from the spacecraft surface is developed. The model, calibrated using ATS-5 plasma data during periods when the satellite was in the earth's shadow, is used to predict potentials on a shadowed, electrically isolated surface at geosynchronous orbit as a function of local time. Potentials are also predicted as the spacecraft moves into and out of the earth's shadow. The results indicate accuracies of ± 800 V over a range of 10,000 V.

DD FORM 1 JAN 73 1473 EDITION OF 1 NOV 65 IS OBSOLETE

Unclassified

SECURITY CLASSIFICATION OF THIS PAGE (When Data Entered)

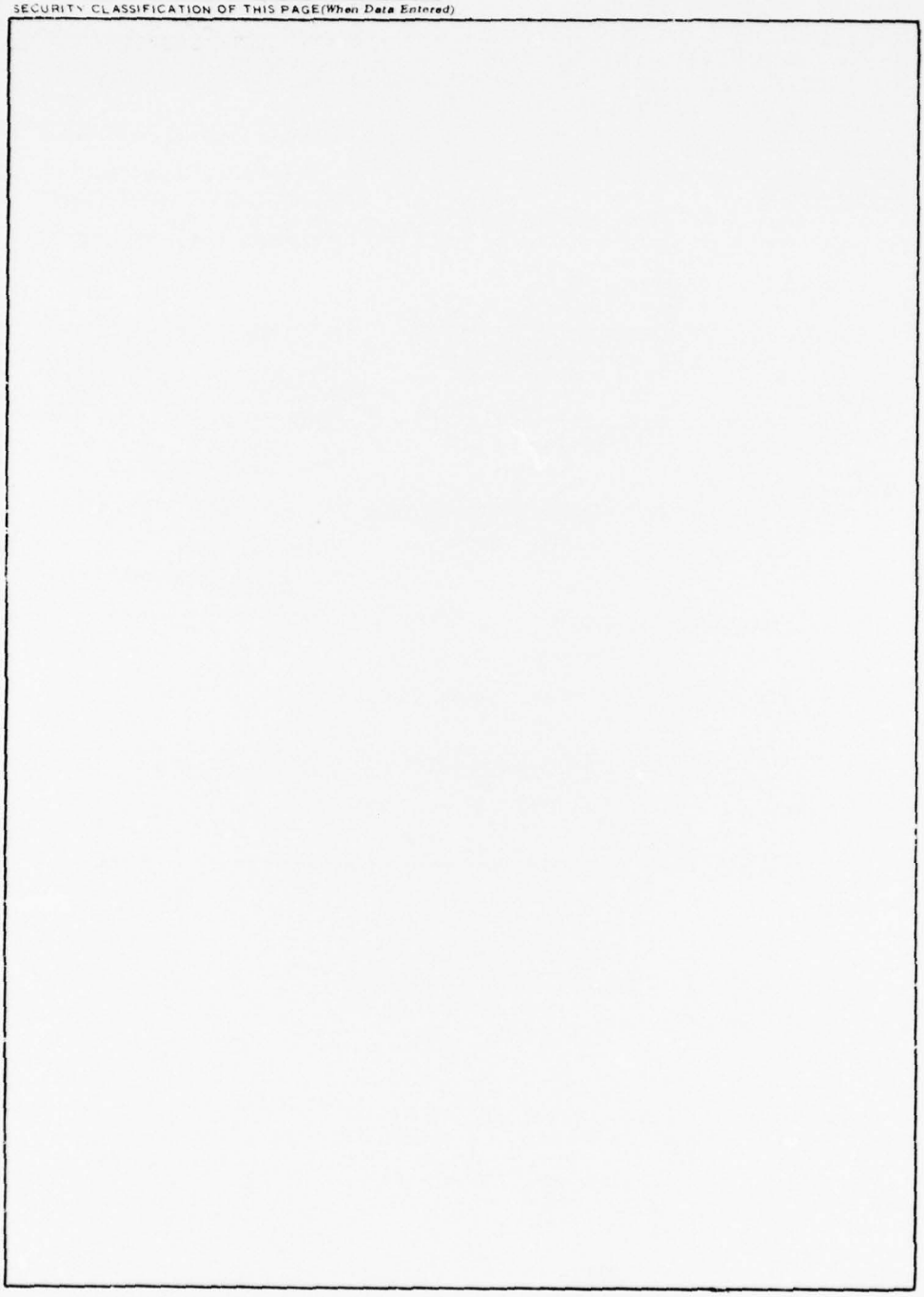

Preface

I would like to thank Dr. S. DeForest for kindly providing his original program listings from which various parts of this study were adapted. Both Dr. W. Burke and C. Pike provided valuable comments on the drafts of this report. Finally, I would like to express my appreciation to Dr. E. C. Whipple for providing a copy of his thesis.

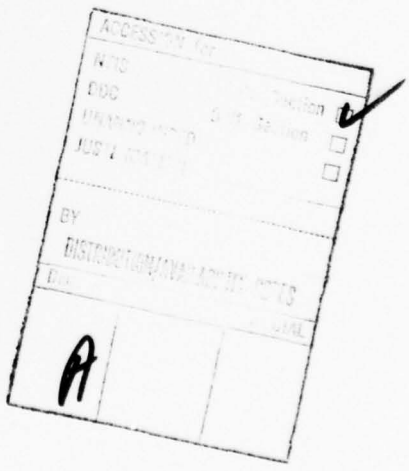

Contents

Illustrations

Tables

Spacecraft Potential Calculations — A Model

1. INTRODUCTION

The calculation of the potential on a satellite immersed in a plasma is, at best, a difficult problem. In particular, the accurate prediction of the potential on a spacecraft in the space environment requires ultimately the simultaneous calculation of the paths of all charged particles in the vicinity of the spacecraft. In principle this is possible, in practice it is not feasible and a variety of techniques have been developed to simplify the problem.[1,2,3,4] Although capable of a fairly accurate treatment both in time and space, these models are limited in usefulness as they require large amounts of computer time or do not include all of the various current sources necessary to simulate the charging phenomenon. This report will present an approximate solution to the problem that yields spacecraft potentials by making assumptions that are equivalent to the "thick sheath" probe solution for a sphere. Though similar models have been developed,[5,6,7,8] none have included the actual measured spectra in their calculations. The model and FORTRAN listings (see Appendix A and B) to be described in this report use actual ATS-5 and ATS-6 data and are adapted from methods originally developed by Whipple and DeForest. (See References 1 and 9.) The model, limited somewhat in its range of applicability

(Received for publication 4 May 1978)

(Because of the large number of references cited above, they will not be listed here. See Reference Page 25 for References 1 through 9.)

to potentials of -10,000 V and plasma temperatures between 50 eV and 30 keV, results in significant savings in computer time over more complicated models.

In the first part of this report the model will be formulated. The individual current sources are presented and approximations as a function of satellite potential developed. The model is calibrated using actual ATS-5 observations of the potential. Two examples will be discussed in which the model is used to study the effects of the time-varying geosynchronous environment and of a time-varying photoelectron flux on spacecraft potential. In Appendix A, we list the FORTRAN programs, and, for the reader new to the field, a brief synopsis of sheath theory is given in Appendix B.

2. MODEL FORMULATION

In solving the spacecraft charging problem we are concerned with finding the spacecraft potential ϕ such that

$$J_e - (J_I + J_{se} + J_{sI} + J_{BSe} + J_{ph}) = 0 \tag{1}$$

where

J_e = Incident electron current,

J_I = Incident ion current,

J_{se} = Secondary emitted electron current due to J_e,

J_{sI} = Secondary emitted electron current due to J_I,

J_{BSe} = Back scattered electron current due to J_e,

J_{ph} = Photoelectron emission (independent of J_e or J_I).

Given the incident ion and electron particle spectra, the currents J_e, J_I, J_{se}, J_{sI}, and J_{BSe} are found and adjusted by varying ϕ on the spacecraft until Eq. (1) holds.

As an example of the calculation of the currents, consider the following. The number flux, $\langle NF \rangle_{eo}$, of electrons at 0 spacecraft potential is, for an isotropic Maxwellian particle distribution,

$$\langle NF \rangle_{eo} = \int_0^\infty (V)\, f_e\, V^2\, dV = \frac{n_e}{2\pi} \left(\frac{2\, k\, T_e}{\pi\, m_e} \right)^{1/2} \tag{2}$$

where

$$f_e(V) = n_e \left(\frac{m_e}{2\pi kT_e} \right)^{3/2} e^{-\frac{m_e V^2}{2kT_e}} \tag{3}$$

m_e = mass of electron,

V = velocity,

n_e = number density of electrons,

kT_e = thermal energy of electrons.

(See Reference 10 for details.) This is equal to J_{eo}, the ambient current, as

$$\langle NF \rangle_{eo} = \frac{J_{eo}}{q\pi} . \tag{4}$$

For no potential, isotropy, and a Maxwellian distribution, Eq. (2) is exact. Once, however, a probe or satellite is placed in the plasma, the distribution function must be altered.

To demonstrate the effects of a potential, assume by Liouville's theorem

$$f(V) = f'(V') . \tag{5}$$

If q is the charge on a particle

$$1/2\, m_e V^2 = \frac{1}{2}\, m_e (V')^2 + q\phi .$$

So for a Maxwellian distribution,

$$f'(V') = e^{-q\phi/kT_e} f(V')$$

where

$$\left(\frac{2|q\phi|}{m_e} \right)^{1/2} \leq V' \leq \infty \text{ for } q\phi < 0 ,$$

$$0 \leq V' \leq \infty \text{ for } q\phi > 0 .$$

For a negative potential ($q\phi > 0$),

$$\langle NF_e(\phi) \rangle = e^{-q\phi/kT_e} \langle NF \rangle_{eo} . \tag{6a}$$

---

10. Garrett, H. B. (1977) Modeling of the Geosynchronous Orbit Plasma Environment, Part I, AFGL-TR-77-0288.

For a positive potential ($q\phi < 0$) the result is more complicated

$$\begin{aligned} \langle NF_e(\phi) \rangle &= \int_0^\infty (V') f'(V') V'^2 dV' \\ &= \int_{\left(\frac{2|q\phi|}{m_e}\right)^{1/2}}^\infty e^{-q\phi/kT_e} f(V') V'^3 dV' \qquad (6b) \\ &= \langle NF \rangle_{eo} \left(1 + \frac{|q\phi|}{kT_e}\right) \end{aligned}$$

or, converting to current

$$J_e(\phi) = \begin{cases} J_{eo} e^{-q\phi/kT_e} & q\phi > 0 \\ J_{eo} \left(1 + \frac{|q\phi|}{kT_e}\right) & q\phi < 0 \,. \end{cases} \qquad (7)$$

At this point it should be noted that Eq. (5) is not entirely correct. In fact, Eq. (7) indicates that as $T \to 0$, for $q\phi < 0$, $J(\phi) \to \infty$. The cause of this error is that in Eq. (5) the detailed distribution function $F(V_x, V_y, V_z)$, for $f(V)$, should have been used (see Appendix B). Along a particle trajectory, Liouville's theorem still holds,

$$F(X, Y, Z, V_x, V_y, V_z) = F'(X', Y', Z', V'_x(\phi), V'_y(\phi), V'_z(\phi)) \,, \qquad (5')$$

where F' is the detailed distribution function at the surface of the satellite. If F is isotropic, F' is not in general isotropic except as an approximation. Further, the integration of F', as in Eq. (6), is extremely difficult for now the velocities V_x, V_y, and V_z are related to V'_x, V'_y, and V'_z by complex formulas. In our model, recognizing that Eq. (5) is inherently inaccurate, we will nonetheless assume it leads to approximately correct results (that is, it yields the results for a thick sheath). Eventually, we will test this assumption by comparing predictions of the model with actual data.

Assuming Eq. (5) to hold, this implies that the distribution function measured at energy E at 0 potential is shifted in energy by $\pm |q\phi|$ depending on the sign of the charge and the satellite potential. Figure 1 illustrates this behavior for a Maxwellian distribution as measured at the spacecraft. Equating $E = 1/2\ m\ V^2$ gives

$$f(E) = \left(\frac{m}{2\pi k}\right)^{3/2} \left(\frac{n}{T^{3/2}}\right) e^{-E/kT} \qquad (8)$$

so

$$\text{Ln}\,(f(E)) = a\,E + b$$

where

$$a = -1/kT$$

$$b = \text{Ln}\left[\left(\frac{m}{2\pi k}\right)^{3/2}\left(\frac{n}{T^{3/2}}\right)\right],$$

hence the linear behavior of Ln (f) vs E.

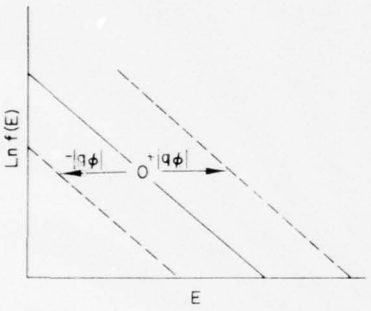

Figure 1. Particle Distribution Function f (assumed to be Maxwellian) vs Energy E For Various Spacecraft Potentials

For a positive (negative) spacecraft potential and for ions (electrons), the particle distribution function is shifted to the left by energy $|q\phi|$ as shown in Figure 1. Particles with energy less than $|q\phi|$ do not reach the spacecraft. Similarly, for a negative (positive) spacecraft potential and for ions (electrons), the particle distribution function is shifted to the right by energy $|q\phi|$. Since no particles exist with $E<0$ initially, the region 0 to $|q\phi|$ is void of particles.

Given the proper integration limits, the problem of calculating J_e, J_I, J_{se}, J_{SI}, and J_{BSe} is reduced to replacing f (E) by $\exp\left(\frac{-q\phi}{kT}\right) f(E)$. In the following sections the integrations leading to J_e, J_I, J_{se}, J_{SI}, and J_{BSe} will be performed using this replacement. Therefore, within the accuracy of the assumption of Eq. (5) (or, equivalently, the thick sheath approximation), these calculations reflect the actual currents to the spacecraft.

Once the currents to and from the spacecraft as a function of ϕ are known, an iterative procedure in which the spacecraft potential is varied is employed to find ϕ such that Eq. (1) is satisfied. A FORTRAN program for accomplishing this is

given in Appendix A along with various programs for calculating the necessary currents. Input is required in the form of the differential energy flux spectrum (obtained for an electrostatic analyzer by multiplying the count rate by a constant) versus energy (62 steps plus one for background corrections are employed in this version). Details of the actual programs, data filtering steps, and extrapolation are covered in the appendices.

3. ELECTRON AND ION INCIDENT CURRENT

In Eq. (6), the formulas necessary to calculate the incident electron and ion currents are given in terms of the distribution function. The ATS-5 satellite, however, employs electrostatic analyzers. Instead of the distribution function as a function of energy, these detectors return the differential energy flux, $\frac{d\,(EF)}{dE}$. Thus, it is convenient to express the integrals in terms of E and $\frac{d\,(EF)}{dE}$ rather than f (V) and V.

The conversion from f to $\frac{d\,(EF)}{dE}$ is given by

$$f = \frac{d\,(EF)}{dE}\,\frac{1/2\ m^2}{E^2} \tag{9a}$$

where the conversion factors (K_e and K_I) are, if f is given in sec^3/km^6, $\frac{d\,(EF)}{dE}$ in $ergs/cm^2\text{-}sec\text{-}sr\text{-}eV$, and E in eV:

$$K_e = 0.1617 \text{ for electrons} \tag{9b}$$

$$K_I = 5.45 \times 10^5 \text{ for ions} \tag{9c}$$

This gives

$$\langle NF_e \rangle = K_e \int_0^\infty \frac{d\,(EF)}{dE}\bigg|_e \frac{dE}{E}\,, \tag{10}$$

$$\langle NF_I \rangle = K_I \int_0^\infty \frac{d\,(EF)}{dE}\bigg|_I \frac{dE}{E}\,,$$

where the results are left in terms of the number flux rather than actual current density J (remember only a multiplication by $q\pi$ is required). The values of $\frac{d\,(EF)}{dE}$ are shifted in potential before the integration by utilization of Eqs. (5) and (9). In the actual case an interpolation is necessary as the desired value of $\frac{d\,(EF)}{dE}$ for the shifted spectrum usually does not correspond to an observed value of $\frac{d\,(EF)}{dE}$.

As the ATS-5 data are for discrete energy bands for the range 51 eV to 51 keV, the integrals become sums (dE becomes ΔE) over this range. Results indicate that these approximations are adequate for a range of 50 eV to 30 keV in temperature and 500 V to -10,000 V in potential.

4. SECONDARY EMISSION CURRENT

Electrons and ions striking the satellite surface are either scattered off the surface or cause the emission of low energy, secondary electrons. Secondary emission is usually given in terms of the incident differential current density, $\frac{dJ_i}{dE}$. This current density is related to $\frac{d(EF)}{dE}$ by

$$\frac{dJ_i}{dE} = \frac{q\pi}{E} \frac{d(EF)}{dE} , \tag{11}$$

(the $q\pi$ factor will be dropped in future discussions).

For secondary emission, the amount of secondary current emitted for a given incident flux is expressed as a ratio $\delta(E)$,

$$\delta(E) = \frac{dJ_s(E)}{dJ_i(E)} \tag{12}$$

where

$\delta(E)$ = the yield function,

$\frac{dJ_s}{dE}$ = the differential secondary current density,

$\frac{dJ_i}{dE}$ = differential incident current density .

The energy spectrum, g(E'), of the secondary electrons is approximately independent of the incident particle energy and, for aluminum, is given in Figure 2.[1] Multiplying g(E') by the secondary current density $J_s(E)$ gives the differential current density of secondary electrons due to particles of energy E as

$$\frac{dJ(E', E)}{dE} = g(E') J_s(E) . \tag{13}$$

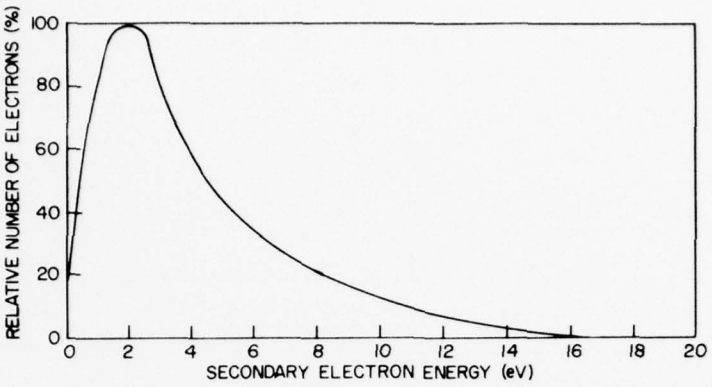

Figure 2. Energy Spectrum For Secondary Electrons

From Eqs. (11) and (12)

$$\frac{d\,J_s(E)}{dE} = \delta(E)\,\frac{dJ_i(E)}{dE} = \frac{\delta(E)}{E}\,\frac{d(EF)}{dE}. \tag{14}$$

This implies that the total current density is given by,

$$\begin{aligned}
J_{TS} &= \int_0^\infty dE' \int_0^\infty dE\, \frac{d^2J(E', E)}{dE'dE}, \\
&= \int_0^\infty dE' \int_0^\infty dE\, \frac{d}{dE}\,\frac{(dJ(E', E))}{dE'}, \\
&= \int_0^\infty dE' \int_0^\infty dE\, \frac{d(g(E')\,J_s(E))}{dE}, \\
&= \int_0^\infty g(E')\,dE' \int_0^\infty \frac{dJ_s(E)\,dE}{dE} \\
&= \int_0^\infty g(E')\,dE' \int_0^\infty \delta(E)\,\frac{dJ_i(E)\,dE}{dE} \\
&= \int_0^\infty g(E')\,dE' \int_0^\infty \delta(E)\,\left[\frac{d(EF)}{dE}\right]\,\frac{dE}{E}.
\end{aligned} \tag{15}$$

The energy spectrum g(E') peaks sharply at ~2 eV and thus for ions and electrons is ~0 if ϕ is greater than + 2 V (all the secondary electrons are attracted) and 1 if ϕ is negative. To the order of accuracy of these calculations

$\int_0^\infty g(E')\,dE'$ will be assumed = 0 for $\phi > 0$ and = 1 for $\phi \leq 0$. From data presented by Whipple[1] $\delta(E)$ is approximated for electrons impacting on aluminum by

$$\delta_e(E) \approx \begin{cases} 0.018\, e^{E/8.31} & E \leq 20 \text{ eV} \\ 0.786 \log_{10} E - 0.823 & 20 \text{ eV} \leq E \leq 100 \text{ eV} \\ 0.18 \sin\left[\pi (\log_{10} E - 2.)\right] + 0.75 & 100 \text{ eV} \leq E \leq 10^3 \text{ eV} \\ -0.45\, (\log_{10} E) + 2.1 & 10^3 \text{ eV} \leq E \leq 2\times 10^4 \text{ eV} \\ 0.34\, e^{-E/28800} & 2\times 10^4 \text{ eV} \leq E\,. \end{cases} \tag{16}$$

The actual curve is shown in Figure 3.

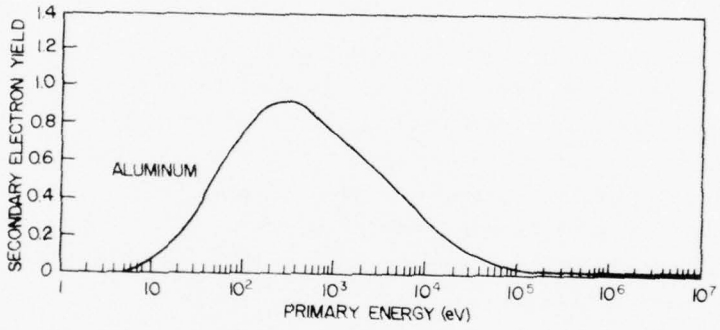

Figure 3. Secondary Electron Yield for Electron Impact on Aluminum

The yield function $\delta(E)$ is not well known for ions impacting on aluminum but a fit to the data presented by Whipple[1] (see Figure 4) indicates that for H^+ and for the energy range of interest*

$$\delta(E) \approx \begin{cases} 0.086 & E \leq 700 \text{ eV} \\ 5 \cdot \exp\left(\frac{-4060}{(E+300)}\right) & 700 \text{ eV} \leq E \leq 10^5 \text{ eV}\,. \end{cases} \tag{17}$$

These values should be used with caution.

* Note: We are only interested in the energy range 0 to 85 keV in this study. The actual curve turns over at 100 keV.

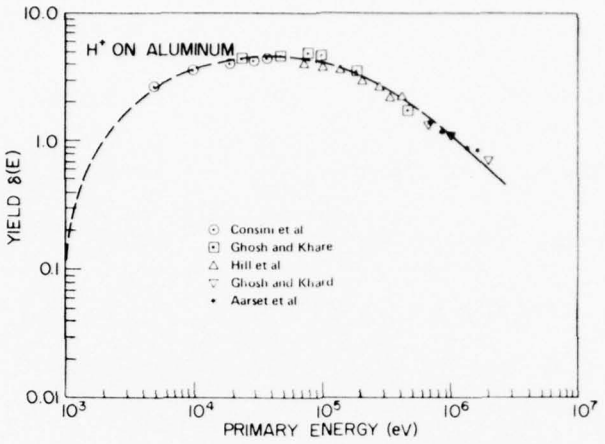

Figure 4. Secondary Electron Yield for Ion (H^+) Impact on Aluminum

The yield function $\delta(E)$ for the incident ions and electrons is substituted into Eq. (15) and integrated using the appropriate shifted values for $\frac{d(EF)}{dE}$ to obtain the secondary emission currents due to the electrons and ions. Typically, the secondary emission due to electrons results in a current of approximately 25 to 50 percent that of the incident electron current while the secondary emission due to ions resulte in an electron current approximately 2 to 3 times that of the incident ions. As will be discussed shortly, it was necessary to adjust these values to obtain accurate estimates of the potential.

5. BACKSCATTERED ELECTRON CURRENT

Some incident electrons are reflected giving rise to the backscattered electron current (the backscattered current due to ions is very small and ignored). Although simple theories of collisional scattering such as those of Everhart[11] are useful in predicting the net current, experimental curves for backscattered emission from aluminum are also available (Sternglass).[12] DeForest[9] has adapted these results to the ATS-5 data. His development, which will be presented here, is similar to that given for secondary electrons.

11. Everhart, T. E. (1960) Simple theory concerning the reflection of electrons from solids, Journal of Appl. Phys. 31(No. 8):1483.

12. Sternglass, E. J. (1954) Backscattering of kilovolt electrons from solids, Phys. Rev. 95:345.

The basic equation for backscattering is

$$J_{BSe} = \int_0^\infty dE' \int_{E'}^\infty B(E', E) \frac{d J_i (E)}{dE} dE \tag{18}$$

where

E' = energy of backscattered particles ($E' \leq E$),

E = energy of incident particles,

$B(E', E)$ = percentage of electrons scattered at a given energy E' as a result of an incident electron at energy E,

$J_i(E)$ = incident current (electrons in this case).

From Sternglass [12]

$$B(E', E) = \frac{G(E'/E)}{E} \tag{19}$$

G is given as a function of $K = E'/E$ (DeForest, private communications) in Figure 5. Numerically, for aluminum

$$G(K) \approx \begin{cases} -0.925\,K + 0.925 & K \geq 0.8, \\ -0.725\,K + 0.765 & 0.6 \leq K \leq 0.8, \\ -0.05\,K + 0.30 & 0.4 \leq K \leq 0.6, \\ -0.5\,K + 0.12 & K < 0.4. \end{cases} \tag{20}$$

(Note: $G(K) \sim \frac{4K}{3}(1-K)$).

For aluminum, when B (E', E) is substituted in Eq. (18), a ratio of ~25 percent for the backscattered current to incident current is obtained in agreement with other estimates.

---

13. Grard, R.J.L., Knott, K., and Pedersen, A. (1973) The influence of photoelectron and secondary electron emission on electric field measurements in the magnetosphere and solar wind, Photon and Particle Interactions with Surfaces in Space, R.J.C. Grard (Ed.) D. Reidel Publishing Co., Dordrecht, Holland, pp 163-189.

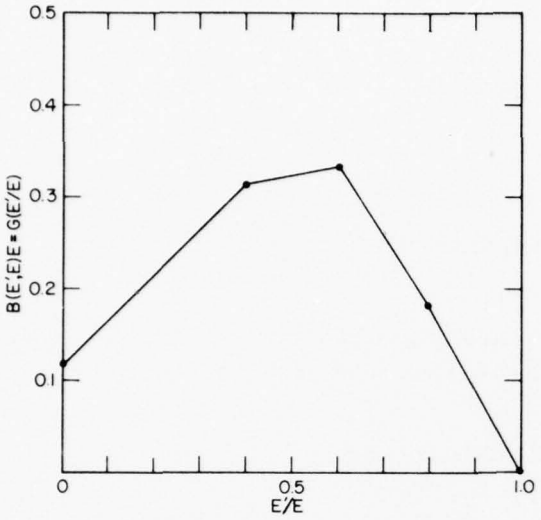

Figure 5. Graph of $B(E', E) \cdot E$ As a Function of (E'/E) Where $B(E', E)$ Is Approximately the Percentage of Electrons Scattered at a Given Energy E' As a Result of an Incident Energy E

Continuing, Eq. (18) becomes

$$J_{BSe} = \int_0^{\infty} \left(\frac{dE'}{E'}\right) \int_{E'}^{\infty} \left[\frac{E'}{E} \; G\left(\frac{E'}{E}\right)\right] \frac{d(EF)}{dE}\bigg|_e \left(\frac{dE}{E}\right). \tag{21}$$

(Note: $\frac{dE'}{E}$ and $\frac{dE}{E} = 0.12$ for ATS-5)

Substituting the proper values of $\frac{d(EF)}{dE}\Big|_e$ in Eq. (21) and performing the integration gives the total current due to backscattered electrons. Unlike the secondary electron current, though, the backscattered current is a gradual function of spacecraft potential. For positive potentials, the 0 integral limit in Eq. (21) should be replaced by $|q\phi|$, the energy shift due to the spacecraft potential.

6. PHOTOELECTRON EMISSION

Light, particularly in the ultraviolet, falling on the spacecraft causes the emission of photoelectrons. Although the characteristics of the emitted particles and the processes involved are well known, the actual photoelectron emission from a spacecraft is poorly known. The reason is the variety of materials on the typical spacecraft surface and the lack of precise knowledge of the solar spectrum and its interaction with various materials. Grard et al[13] and Whipple[1] have combined the solar

spectrum with the emission characteristics of various substances to give the photoelectron current as a function of energy. DeForest (private communication) has developed an algorithm that approximates their results. It gives the photoelectron current as a function of positive spacecraft potential (for negative potential all of the photoelectron current leaves the spacecraft). It is

$$J_{ph} = \frac{J_{po}}{(\phi/0.7 + 1)^2} \qquad \phi > 0 \ . \tag{22}$$

Values for J_{po} are given in Table 1. From this table it is clear that estimates of J_{po} range over an order of magnitude. Fortunately, most examples of charging that we will be concerned with involve shadowed surfaces in which case $J_{po} = 0$. The charging model will, however, in conjunction with actual data, be used in a later section to estimate the value of J_{po} appropriate to ATS-5.

Table 1. Values for J_{po}

Author	Saturation Current (n A/cm^2)	
Grard et al[13]	4.20	(Aluminum oxide)
	3.00	(Indium oxide)
	0.40	(Graphite)
DeForest[9]	0.82	(ATS-5)
Whipple[1]	3.00	(Rocket-aluminum)

7. COMPARISON WITH DATA

The ultimate check of any model is how well the predicted results compare with actual measurements. The basic set of data will be spectra from ATS-5 for periods immediately before and after entry into the earth's shadow and for periods immediately before and after exit from the earth's shadow. These periods were selected as they can be used not only to study large potential variations (on the order of ~6 kV) but also to calibrate the photoelectron flux. Table 2 lists the eclipses studied and the observed potentials during eclipse.

Table 2. Eclipses Studied

Date		UT	Potential
1969	22 Sep	0629	-3400
		0731	-3810
	16 Oct	0627	-5360
		0711	-3810
1970	12 Sep	0631	-2420
		0718	-1730
	15 Sep	0626	-877
		0721	-1540
	17 Sep	0623	-5380
		0723	-3040
	19 Sep	0620	-2720
		0724	-1940
	26 Sep	0724	-2170
	17 Oct	0630	-1230
		0659	-2170
	18 Oct	0633	-397
		0650	-316
	19 Oct	0640	-396
		0648	-558

ATS-5 does not consist of a single material nor can it be said to be spherical in shape (a tacit assumption in the preceding analysis). However, keeping to the spirit of a "simple" charging model, the satellite was approximated as an aluminum sphere. Figure 6 shows the results of these calculations. The discrepancies between observed and predicted potentials have been corrected by adjusting the coefficients of the secondary emission terms to give a best fit in a least squares sense (the backscattered flux correlates so well with the incident electron flux that determining its coefficient is somewhat difficult as it may reflect slight errors in the actual measurement of J_e). For correction factors of 1.3 (J_{se}), 0.55 (J_{sI}), and 0.4 (J_{BS}), the results have a standard deviation of ± 800 volts. It should be kept in mind, though, that the model is based on several assumptions and, considering these, this agreement is quite good.

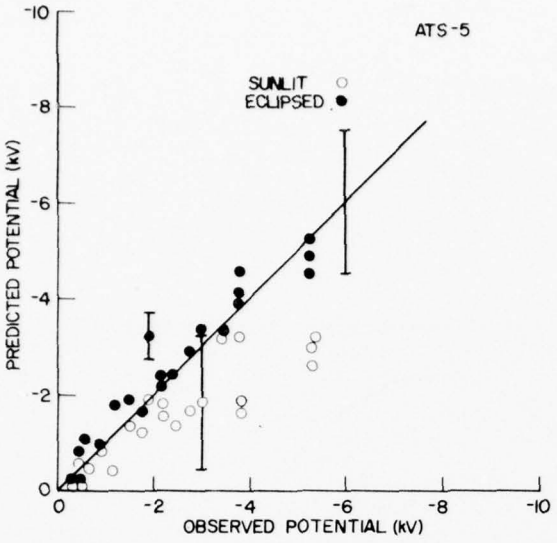

Figure 6. Predicted vs Observed Potentials. The results for spectra when the satellite was illuminated and when it was shadowed are given

8. MODEL APPLICATION

The model has been developed for two purposes. First, combined with the geosynchronous plasma model developed by Garrett,[10] it can be used to predict potentials on spacecraft as a function of the geomagnetic index A_p and LT, the satellite local time. It also is employed to calculate the potential on a spacecraft as it passes into and out of the earth's shadow.

Figure 7 plots the potential variations predicted by the model for the geosynchrous simulation model of Garrett[10] for moderate geomagnetic activity (A_p = 120) and high geomagnetic activity (A_p = 1656). That simulation gives a "2 Maxwellian fit" to the plasma such that the distribution functions are for electrons

$$f_e(E) = 27.2\,(N1_e \left(\frac{T1_e}{1000}\right)^{-3/2} e^{-E/T1_e} + N2_e \left(\frac{T2_e}{1000}\right)^{-3/2} e^{-E/T2_e} \quad (23a)$$

and for ions

$$f_I(E) = 2.14\times 10^6\,(N1_I \left(\frac{T1_I}{1000}\right)^{-3/2} e^{-E/T1_I} + N2_I \left(\frac{T2_I}{1000}\right)^{-3/2} e^{-E/T2_I} \quad (23b)$$

where

$N1_e$, $N2_e$ = electron number densities (n/cm^3),

$T1_e$, $T2_e$ = electron temperatures (eV),

$N1_I$, $N2_I$ = ion number densities (n/cm^3),

$T1_e$, $T2_I$ = ion temperatures (eV).

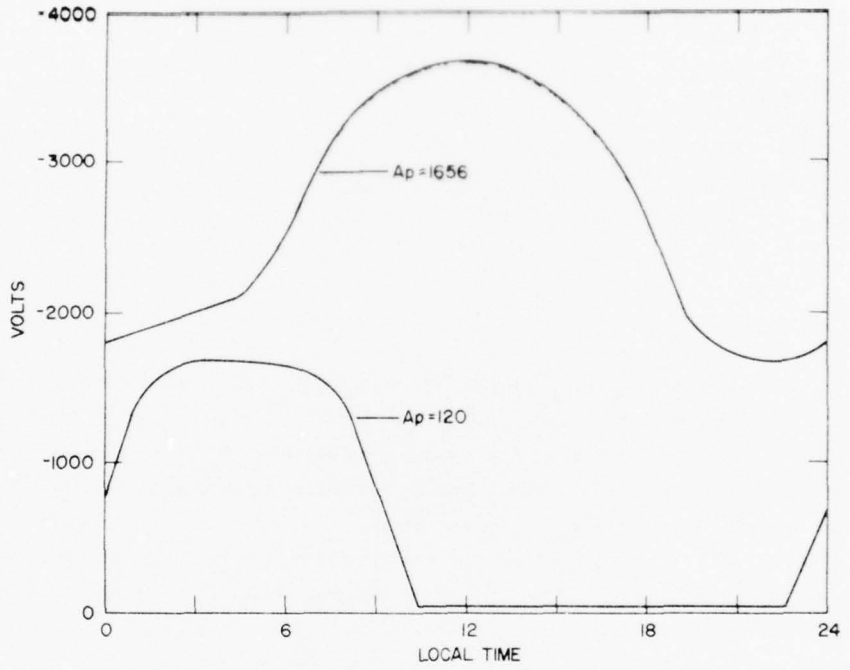

Figure 7. Predicted Potential of a Shadowed, Electrically Isolated Surface as a Function of Local Time

The distribution functions are converted to differential energy spectra using Eq. (9). The spectra are inserted into the program and, assuming no photoelectron current, the potential calculated. These potentials are the maximum that would be expected for a shadowed, electrically isolated surface as a result of the ambient environment.

Another use of the model is in the determination of the potential as a spacecraft passes into the earth's shadow. The eclipse data described earlier are used to determine the photoelectron flux necessary to give the observed potential variations as ATS-5 passed into and out of the earth's shadow. By varying the amplitude of an

appropriate model of atmospheric attenuation to fit the observed photoelectron current, J_{po} was found. The resulting value was determined to be 0.4 n A/m^2 which is in agreement with the values in Table 1. The reader is referred to Garrett[14] for details of this procedure.

Figure 8 shows the observed and predicted potentials as ATS-5 passes into and out of eclipse on 17 September 1970. The results of the prediction are adequate and within the ± 800 V error but their deviations from the observed values may indicate either a need to include sheath effects or that the thick sheath, spherical probe approximation is inaccurate. In any event, this method of testing, by comparing the observed and predicted potentials as the photoelectron flux is varied, should prove to be a powerful tool for comparison with other spacecraft charging models in the future.

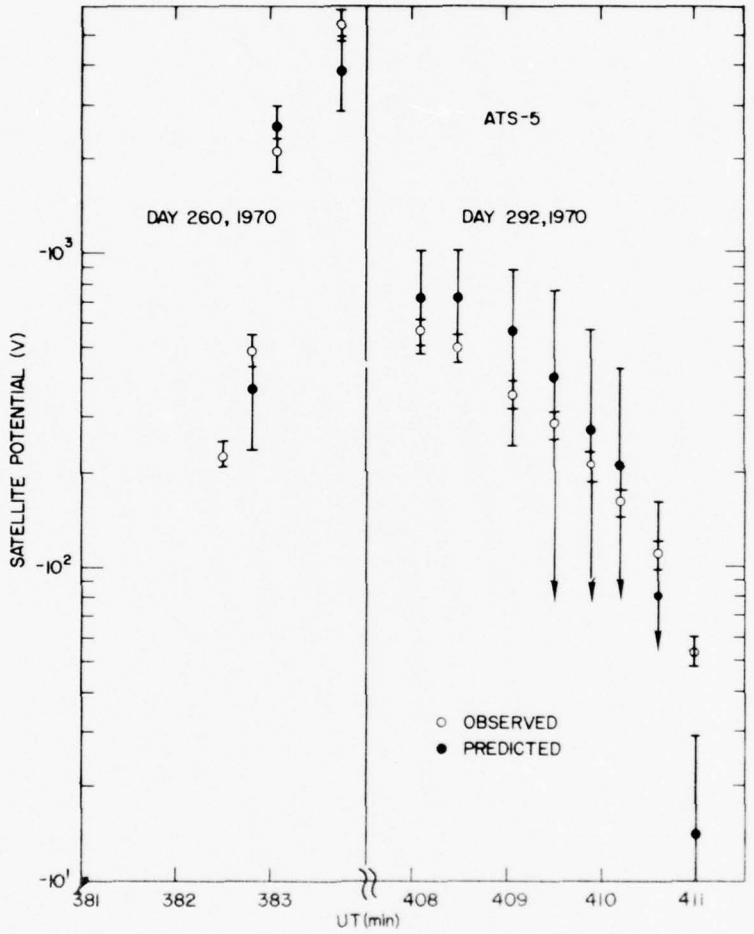

Figure 8. Comparison of Observed and Predicted Potentials on the ATS-5 Satellite as a Function of Time. Upper limits are potentials predicted by eclipse spectra, lower limits are potentials predicted by illuminated spectra, and central value 0's the average of the two

14. Garrett, H. B. (1978) Effects of a Time-Varying Photoelectron Flux on Spacecraft Potential, AFGL-TR-78-0119.

9. CONCLUSION

A simple model based on the work of Whipple[1] and DeForest[9] has been developed. The model was calibrated with ATS-5 plasma data. The model predictions for the potential on a satellite as it passed into eclipse were compared with actual observations. The results indicate agreement between the predicted and observed values. The model is used in conjunction with a model simulation of the geosynchrous environment to predict spacecraft potentials under different geomagnetic and local time conditions. The model, after being calibrated, successfully predicts potentials with ±800 V accuracy over a range of 10,000 V. It includes relevant current terms and is efficient in comparison with other more complex models, taking ~2 sec per potential calculation. A FORTRAN listing of the program is provided in Appendices A and B. For reference, a simple theory of the plasma sheath is also presented.

References

1. Whipple, E. C. (1965) The Equilibrium Electric Potential of a Body in the Upper Atmosphere, NASA X-615-65-296.

2. Rothwell, P. L., Rubin, A. G., and Yates, G. K. (1977) A simulation model of time-dependent plasma-spacecraft interactions, Proc. of the Spacecraft Charging Conference, AFGL-TR-77-0051/NASA TMX-73537.

3. Laframboise, J. G., and Prokopenko, S. M. L. (1977) Numerical simulation of spacecraft charging phenomena, Proc. of the Spacecraft Charging Conference, AFGL-TR-77-0051/NASA TMX-73537.

4. Parker, L. W. (1977) Calculation of sheath and wake structure about a pill-box-shaped spacecraft in a flowing plasma, Proc. of the Spacecraft Charging Conference, AFGL-TR-77-0051/NASA TMX-73537.

5. Rosen, A. (1975) Spacecraft Charging: Environment Induced Anomalies, Paper 75-91, AIAA 13th Aerospace Sciences Meeting, 1975.

6. Massaro, M. J., Green, T., and Ling, D. (1977) A charging model for three-axis stabilized spacecraft, Proc. of the Spacecraft Charging Conference, AFGL-TR-77-0051/NASA TMX-73537.

7. Inouye, G. T. (1976) Spacecraft potentials in a substorm environment, Spacecraft Charging by Magnetospheric Plasma, AIAA Progress in Astronautics and Aeronautics Series, Vol 42, Rosen (Editor).

8. Purvis, C. K., Stevens, N. J., and Oglebay, J. C. (1977) Charging characteristics of materials: comparison of experimental results with simple analytical models, Proc. of the Spacecraft Charging Conference, AFGL-TR-77-0051/NASA TMX-73537.

9. DeForest, S. E. (1972) Spacecraft Charging at Synchronous Orbit, J. Geophys. Res. 77(No. 4):651.

10. Garrett, H. B. (1977) Modeling of the Geosynchronous Orbit Plasma Environment, Part I, AFGL-TR-77-0288.

11. Everhart, T. E. (1960) Simple theory concerning the reflection of electrons from solids, Journal of Appl. Phys. 31(No. 8):1483.

12. Sternglass, E. J. (1954) Backscattering of kilovolt electrons from solids, Phys. Rev. 95:345.

13. Grard, R. J. L., Knott, K., and Pedersen, A. (1973) The influence of photoelectron and secondary electron emission on electric field measurements in the magnetosphere and solar wind, Photon and Particle Interactions with Surfaces in Space, R. J. C. Grard (Ed.) D. Reidel Publishing Co., Dordrecht, Holland, pp 163-189.

14. Garrett, H. B. (1978) Effects of a Time-Varying Photoelectron Flux on Spacecraft Potential, AFGL-TR-78-0119.

15. Chen, F. F. (1965) Electric Probes, Plasma Diagnostic Techniques, R. H. Huddestone and S. L. Leonard (Eds.) Academic Press, Inc., New York, New York, pp 113-200.

Appendix A

FORTRAN Listings

The solution of Eq. (1), the current balance equation, involves an iterative procedure with three steps. Once the input data are properly filtered, the interation commences with a computation of the currents assuming the initial potential to be 0. The currents are combined as in Eq. (1) and the deviation from 0 current calculated. Depending on whether the deviation is close to 0 or not, the process is either terminated or a new potential estimated. The spectra are shifted by the new potential and the process repeats. (See flow chart at end of this Appendix.)

As the determination of the energy, E, and of the corresponding differential energy flux, $\frac{d\,(EF)}{dE}$, for the electrons and ions is satellite dependent, we will not discuss this aspect. The program as currently arranged accepts an energy spectrum having N steps. The first step is assumed to be 0 energy and contain the background counting rates. The subroutine listings using this as input follow Appendix B.

The data from a real satellite are usually not continuous. Subroutine FIL is designed to take the data, interpolate missing points, drop values below background or below the satellite potential (particles having energy less than the spacecraft potential are trapped and do not contribute to the satellite current) and, if desired, estimate values outside the energy range of the instrument. In the current form the program ignores all channels having 0 or negative energy flux until the first non-zero channel is reached. After this channel, all missing values are interpolated using a linear approximation. If the last channel is zero, it will be left zero. The

program expects N values of the differential energy flux in array C1 (electrons) and C2 (ions) in units of eV/(cm^2-sr-sec-eV). V is the satellite potential when the measurements were made (held in common).

Subroutine SHIFT takes as input C1, C2, and E. It also needs the number of points, M, and the satellite number (important only for ATS-5). The potential at which the spectra were determined (that is, spacecraft potential) is VS. The potential to which the spectra are to be shifted is V0. The new values of C1 and C2 are found by first determining the energy in the unshifted spectrum corresponding to the new, desired (shifted) energy. S1 (or S2), the shifted value, is determined by interpolating between the values of C1 (or C2) corresponding to the energies bracketing the unshifted energy. Using Liouville's theorem, this interpolated value is shifted to the new energy, E_s, by dividing it by the square of the ratio of the unshifted energy, E_o, to the new energy

$$S1\,(E_s) = C1\,(E_o)\,(E_s/E_o)^2 \,. \tag{A1}$$

The results of SHIFT are input to subroutine DIFI where the individual currents are calculated. The incident currents due to the electrons (FE) and ions (FI) are calculated in TOTAL according to Eq. (10) and returned in X(1) and X(2) (all currents are in n/(cm^2-sec-sr) rather than n A/cm^2). TOTAL requires function D(E, I), where E is the energy array and I is the energy step for which D is to be found. D is the ratio $\frac{\Delta E(I)}{E(I)}$. $\Delta E(I)$ is the energy channel width for a detector. Although function D is satellite dependent (as an example, on ATS-5 $\Delta E/E = 0.12$), it can be generalized if the number 63 in card 16 is changed.

The backscattered flux is calculated in BACK. The total current, assuming 0 or negative potential, is returned along with the backscattered current as a function of positive potential (DBSF). Similarly, the secondary currents due to the electrons (SEF is total) and ions (SPF is total) are returned in X(1) and X(2) by subroutine SEC.* The photoelectron flux is calculated in DIFI according to Eq. (22). The backscattered current is returned in X(5), the secondary current due to electrons in X(3), the secondary current due to ions in X(4), and the photoelectron current in X(6).

---

*The secondary flux due to ions is not accurate above 100 keV.

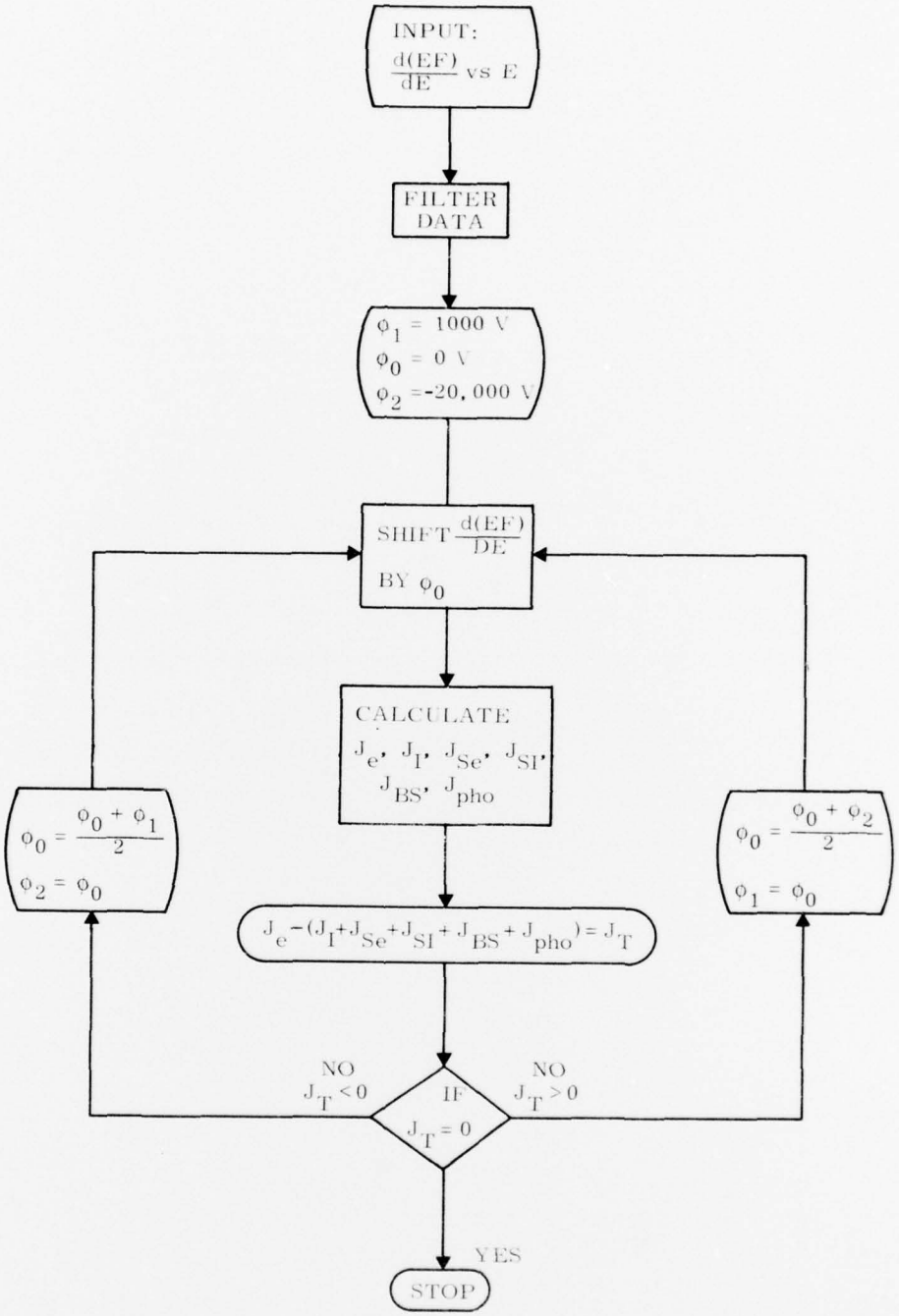
INPUT:
d(EF)/dE vs E
FILTER DATA
φ1 = 1000 V
φ0 = 0 V
φ2 = -20.000 V
SHIFT d(EF)/DE BY φ0
CALCULATE
Je, JI, JSe, JSI, JBS, Jpho
Je − (JI + JSe + JSI + JBS + Jpho) = JT
IF JT = 0
NO JT < 0
NO JT > 0
φ0 = (φ0 + φ1)/2
φ2 = φ0
φ0 = (φ0 + φ2)/2
φ1 = φ0
YES
STOP

Appendix B

Sheath Theory

The measurement of the characteristics of a contained plasma in the laboratory is, in conception, quite simple. Basically, a probe (a wire for example) is placed in the plasma. The potential on the probe is varied and the resulting current measured. A typical current vs voltage curve is shown in Figure B1. As in most respects, the probe problem is identical with that of a satellite immersed in a plasma, our discussion will begin with a description of probe theory.

Qualitatively, if the ion and electron plasma populations can be described by a Maxwellian particle distribution, Figure B1 can be readily interpreted as follows. Referring to the figure in region A, the ion current is collected and the electron current repelled if the probe potential is negative. In region B the electron current is only weakly repelled by the probe potential. At the border between region B and C, the ion and electron currents are, in fact, equal (this corresponds to the spacecraft charging problem). In region C the electron current dominates the ion current (Note: as the electrons are 1800 times less massive, for the same energy they move ~40 times faster than the ions so the electron current is ~40 times larger). In region D almost all the ion current is repelled and the electron current saturates. The exact curves for all these regions are dependent on the temperatures and densities of the ions and electrons.

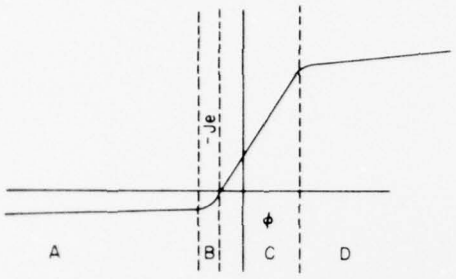

Figure B1. Probe Current (J_e) vs Potential ϕ For a Spherical Probe Immersed in a Neutral, Maxwellian Plasma

This simple picture neglects one important problem—the sheath. As either the ions or electrons dominate the current, they form a cloud in the vicinity of the probe and can drastically alter the calculation of the currents shown in Figure B1. To obtain a better description of the sheath region, consider the following. Assume that the electrons are in thermal equilibrium above a charged plate (that is, assume they form an "atmosphere" with gravity replaced by the electric field):

$$n_e(X) = n_o \, e^{\frac{|q|\phi(X)}{kT_e}} \tag{B1}$$

where

n_o = number density of electrons at surface of plate,

n_e = number density of electrons as a function of X,

X = height above charged plate (X = 0 at plate surface),

ϕ = potential (assumed positive),

q = electron charge

kT_e = thermal energy of electrons.

Further, assume that the ions are motionless and uniformly distributed. By Poisson's equation

$$\frac{d^2\phi}{dX^2} = -4\pi|q|\,(n_i - n_e)\,, \tag{B2}$$

where

n_i = number density of ions.

Substituting in for n_i ($n_i(x) \approx n_o$) and n_e, for small $\frac{|q|\phi}{kT_e}$

$$\frac{d^2\phi}{dX^2} = -4\pi|q|n_o\,(1 - e^{\frac{|q|\phi}{kT_e}})$$

$$\simeq 4\pi|q|n_o\,(|q|\phi/kT_e)\,. \tag{B3}$$

Thus

$$\phi = \phi_o\, e^{-(x/\lambda_o)} \tag{B4}$$

where

$$\lambda_o = \left(\frac{kT_e}{4\pi q^2 n_o}\right)^{1/2} = \text{Debye length,}$$

ϕ_o = potential at plate surface .

This distance (the Debye length) is the distance from the probe over which the probe potential is attenuated by 1/e and is the distance over which the probe potential disturbs the plasma. This is usually called the sheath region.

The sheath region around the probe, particularly if it is large, can significantly alter the shape of the curve shown in Figure B1. Within it, particles are influenced by the changing probe electric field and detailed single particle orbit calculations are often necessary. In space the number densities are quite low ($\lesssim 100/cm^3$) and the temperatures often on the order of 20 keV making the Debye length (or, approximately, the sheath region) on the order of tens of meters. The plasma is, however, collisionless—somewhat simplying the computations.

The effects of particle orbits within the sheath can be seen in the following. Assuming a thick sheath (that is, that $\lambda_o >> r_s$, where r_s is the radius of the satellite), consider a particle having initial kinetic energy $\frac{1}{2} m V_o^2$ and approaching the probe within a distance r. Then, by conservation of energy and angular momentum

$$\frac{1}{2} m V_o^2 = \frac{1}{2} m V_r^2 + q\phi (r),$$

$$m R V_o = m r V_r , \tag{B5}$$

where the $q\phi$ is the potential energy (0 at infinity) and m is the mass of the particle. Solving for the impact parameter R

$$R^2 = r^2 \left(1 - \frac{q\theta (r)}{\left(\frac{m V_o^2}{2}\right)}\right) \tag{B6}$$

Therefore, the total current density at the surface of a spherical probe of radius r_s is, for a monoenergetic particle population, approximately

$$J = \frac{I}{4\pi r_s^2} = J_o \left(1 - \frac{q\phi}{\left(\frac{m V_o^2}{2}\right)}\right) \tag{B7}$$

where

$$J_o = \frac{q n V_o}{4\pi R^2},$$

= the current per unit area,

= ambient density at R.

This follows as any particle which would normally pass through a volume of radius R would, in the presence of a potential ϕ, pass through the volume of radius r_s (assumed to be the spacecraft surface). This would give a current $I = 4\pi R^2 J_o$ at R.

For a Maxwellian distribution, Eq. (B7) becomes[15]

$$J = \frac{I}{A} \approx J_o \left(1 + \frac{|q\phi|}{kT}\right)$$

where kT has replaced $\frac{1}{2} m V_o^2$ and

$$J_o = \frac{1}{2} \pi n \left(\frac{2 k T}{\pi m}\right)^{1/2} .$$

See Eq. (1) in Reference 10.

15. Chen, F.F. (1965) Electric Probes, Plasma Diagnostic Techniques, R.H. Huddestone and S.L. Leonard (Eds.) Academic Press, Inc., New York, New York, pp 113-200.

This result is only applicable for $\lambda_o >> r_s$, the thick sheath approximation, and for a sphere (see Chen[14] for details of this development).

These results for the spherical thick sheath approximation are equivalent to the model presented in this report. As described, explicit assumptions about the nature of the ambient plasma-spacecraft interaction are made that result in an expression [Eq. (7)] identical with that for a spherical thick sheath.

Finally, as discussed in detail in Reference 10 the plasma distribution function, $F(X, Y, Z, V_x, V_y, V_z)$ (where X, Y, Z are spatial coordinates and V_x, V_y, V_z are velocity components) is the conventional basis for describing a space plasma. This function was simplified by assuming an isotropic, collisionless plasma which gives:

$$F(X, Y, Z, V_x, V_y, V_z)\, dx dy\, dz\, dV_x\, dV_y\, dV_z = f(X, Y, Z, V)\, dx\, dy\, dz\, (4\pi V^2 dV)$$

where

$$V = (V_x^2 + V_y^2 + V_z^2)^{1/2}.$$

As discussed in the text, this is an approximation and must be used with care.

```
      SUBROUTINE DIF1(C1,C2,E,X,N,ISAT,V)
      DIMENSION X(6)
      DIMENSION C1(63),C2(63),E(63)
      DIMENSION PEF(64),SEF(63),SPF(63),DBSF(64),BS(64)
      COMMON/UNIT/M,IST
      COMMON/THD/PE
      IST=ISAT
      M=N
      PTT=PE
      CALL TOTAL(C1,C2,FE,FI,E)
      CALL BASE(E,C1,DBSF,BS)
      IF(V.GT.0.0) 2,3
    3 CALL SECT(E,C1,C2,SFPT,SFET,SPF,SEF)
      BSS=BS(2)
      GO TO 4
    2 SFPT=SFET=0
      DO 5 I=2,63
      IH=I
      IHL=I-1
      IF(V.LT.E(IH).AND.V.GE.E(IHL)) 6,5
    5 CONTINUE
    6 BSS=BS(IH)
      IF(V.LE.E(2)) BSS=BS(2)
      PTT=PE/((V/.7)+1.)**2
    4 X(1)=FE
      X(2)=FI
      X(3)=SFET
      X(4)=SFPT
      X(5)=BSS
      X(6)=PTT
   00 FORMAT(7(2X,E10.4))
      RETURN
      END
```

```
      SUBROUTINE SHIFT(C1,C2,E,S1,S2,V0,M,ISAT)
      DIMENSION C1(1),C2(1),E(1),S1(1),S2(1)
      COMMON/ COM3/MM,ISS
      COMMON/VOLT/VS
      RHOI=1
      RHOF=1
      MM=M
      ISS=ISAT
      V=V0-VS
      S1(1)=S2(1)=0
C     ELECTRONS
C     ORIGINAL ENERGY BEFORE SHIFT IS EE
      DO 1 N=2,MM
      EE=E(N)-V
      IF(EE.LT.E(2)) 2,6
    2 S1(N)=0
      GO TO 1
C     FIND FLUX AT EE
    6 DO 3 I=3,M
      IH=I
      IHL=I-1
      IF(EE.LT.E(IH).AND.EE.GE.E(IHL)) 4,3
    3 CONTINUE
    4 CET=C1(IHL)+(C1(IH)-C1(IHL))*(EE-E(IHL))/(E(IH)-E(IHL))
C     AS DISTRIBUTION FUNCTION CONSTANT IN PHASE SPACE=
      S1(N)=RHOI*E(N)*E(N)/(EE*EE)
    1 CONTINUE
C     IONS
C     ORIGINAL ENERGY BEFORE SHIFT IS EP
      DO 11N=2,MM
      EP=E(N)+V
      IF(EP.LT.E(2)) 12,16
   12 S2(N)=0
      GO TO 11
C     FIND FLUX AT EP
   16 DO13 I=3,M
      IH=I
      IHL=I-1
      IF(EP.LT.E(IH).AND.EP.GE.E(IHL)) 14,13
   13 CONTINUE
   14 CET=C2(IHL)+(C2(IH)-C2(IHL))*(EP-E(IHL))/(E(IH)-E(IHL))
C     AS DISTRIBUTION FUNCTION CONSTANT IN PHASE SPACE=
      S2(N)=CET*E(N)*E(N)/(EP*EP)
   11 CONTINUE
      DO 15 I=2,63
      IF(S1(I)-T.0.0) S1(I)=0.0
   15 IF(S2(I)-T.0.0) S2(I)=0.0
      RETURN
      END
```

```
      SUBROUTINE TOTAL (C1, C2, FE, FP,E)
C  CALCULATE TOTAL ELECTRON, FE, AND TOTAL ION FLUX, FP,
C  GIVEN C1 AND C2
      DIMENSION E(1)
      DIMENSION C1(1), C2(1)
      FP=FE=0.0
C  SUM FLUXES
      DO 111 I=2,53
      FP=FP+C1(I) *D(E,I)
  111 FE=FE+C1(I)      *D(E,I)
C  CORRECT FOR ENDS
C     FP=FP+3.*(C2(2)+C2(63))*D(E,I)
C     FE=FE+3.*(C2(2)+C2(63))*D(E,I)
C     FE=FE+1.*(C2(2)+C2(63))*D(E,I)
C     FP=FP+1.*(C2(2)+C2(63))*D(E,I)
      RETURN
      END
```

```
      FUNCTION D(E,I)
      DIMENSION E(1)
      COMMON/NUMB/N,ISAT
C     SETUP D(ITA ENERGY/ENERGY
      K=I+1
      IF(K.EQ.N) D=(E(N)-E(N-1))*2./(E(N)+E(N-1))
      IF(K.EQ.N) GO TO 30
      IF(K.GT.N) D=0
      IF(K.GT.N) GO TO 30
      IF(I.EQ.2) D=(E(K)-E(I))*2./(E(K)+E(I))
      IF(I.EQ.2) GO TO 30
      J=I-1
      D=(E(K)-E(J))/(2.*E(I))
      D=2.*(E(K)-E(J))*(E(K)-E(I))/((E(K)-E(J))*E(I))
      IF(ISAT.EQ.5)D=.12
      IF(ISAT.EQ.5.AND.N.NE.53)D=.24
   30 CONTINUE
      RETURN
      END
```

```
      SUBROUTINE BACK(E,C1,DBSF,BS)
C  CALCULATES INTEGRALS OF BACK-SCATTERED ELECTRONS GIVEN
C  ELECTRON FLUX C1
      DIMENSION C1(1), RI(63),BS(64) ,DBSF(64),W(63,63),F(63)
      BS(64)=0
      DO 46 I=1,63
      DO 46 J 1,63
   46 W(I,J)=0.J
      DO 51 I = 2,62
      IP = I+
      DO 51 J = IP,63
      FK=E(I) /E(J)
      IF(FK    .LT..8)52,53
   52 IF(FK    .LT..6)54,55
   54 IF(FK    .LT..4)57,58
   53 F= FK*(1..325*FK+.925) $ GO TO 51
   55 F=FK*(-.1725*FK+.765)  $ GO TO 51
   58 F=FK*(  .05*FK+.30)    $$ GO TO 51
   57 F= FK*(  F*F( +.12)
   51 W(I,J)=W(E,I)*F
      DO 101 I = 2,63
      I = 65-I $ IP = I+1
      SUM = 0.
      IF(IP.GE.64) GO TO 103
      DO 102 J = IP,63
  102 SUM = SUM + W(I,J)*C1(J)
  103 DBSF(I) = SUM
  101 BS(I)  = BS(IP)+DBSF(I)*D(E,I)
      RETURN
      END


      SUBROUTINE SEC(E,C1,C2,SFPT,SFET,SPF,SEF)
C  CALCULATE SECONDARY ELECTRON FLUXES GIVEN PARTICLE ENERGY
C  E, ENERGY FLUXES C1 AND C2.GIVES FLUX SFPT FOR IONS AND
C  SFET FOR ELECTRONS
C       GARRETT
      DIMENSION E(1), C1(1), C2(1), SPF(63), SEF(63)
      SFPT=SFET=0.
      DO 105 I=2,63
C  COEFFICIENTS FOR IONS:
      GAM=.085
      IF(E(I).GT.700.)  GAM=5.*EXP(-4060./(E(I)+300.))
      SPF(I)=GAM*C2(I)
      SFPT=SFPT+SPF(I)*D(E,I)
C  COEFFICIENTS FOR ELECTRONS
      PI=3.1415
      IF(E(I).LE.20.)   GAM=.018*EXP(E(I)/8.31)
      IF(E(I).GT.20.)  GAM=.786*ALOG10(E(I) ) -.823
      IF(E(I).GT.100.)  GAM=.18*SIN(PI*(ALOG10 (E(I))-2.))+.75
      IF(E(I).GT.1000.)  GAM=-.45*ALOG10(E(I))+2.1
      IF(E(I).GT.21000.)  GAM=.34*EXP(-E(I)/28800.)
      SEF(I)=.A4*C1(I)
      SFET=SFET+SEF(I)*D(E,I)
  105 CONTINUE
      RETURN
      END
```

```
      SUBROUTINE FIL(C1,C2,E,N)
C     GIVEN C1 AND C2, SMOOTHS SPECTRA WHERE C1 AND C2 ARE ELECTRON
C  AND ION EN ERGY FLUX IN EV/(CM**2*SR*SEC*EV)
C     EXPECTS  1 TO BE BACKGROUND AND COUNTS IN 2 THRU N
      DIMENSION C1(1),C2(1)
      DIMENSION E(1)
      COMMON/ C_T/V
      DO 11 I=2,N
C  CORRECT FOR BACKGROUND
      C1(I)=C1(I)-C1(1)
      C2(I) = C2(I)-C2(1)
C  CORRECT ANY NEGATIVE VALUES
      IF(C1(I) .LT.0.)C1(I) = 0.
      IF(C2(I) .LT.0.)C2(I) = 0.
C  IF POTENTIAL IS NEGATIVE, ION COUNT RATES 0 BELOW POTENTIAL
      IF (E(I) .LT.-V) C2(I)=0.0
C  IF POTENTIAL IS POSITIVE, ELECTRON COUNT RATES 0 BELOW POTENTIAL
      IF (E(I) .LT.V) C1(I)=0.0
   11 CONTINU
C  INTERPOLATE J VALUES
      L=N-1
      J=2
      GO TO 4
      IF(E(2).LT.V) GO TO 4
      IF(C1(2 .EQ.0.0) 3,4
    3 J=J+1
      IF(C1(J).EQ.0.0) GO TO 3
      C1(2)=C1(J)
    4 J=2
      GO TO 5
      IF(E(2).LT.-V)GO TO 6
      IF(C2(2).EQ.0.0) 5,6
    5 J=J+1
      IF(C2(J) .EQ.0.0) GO TO 5
      C2(2)=C2(J)
    6 DO 8 I=3,L
      IF(E(I).LT.V) GO TO 8
      J=I
      IF(C1(I) .EQ.0.0) 7,8
    7 J=J+1
      IF(C1(J).EQ.0.0. AND. J.NE.N)  GO TO 7
      M=I-1
      C1(I)=(C1(J)-C1(M))*(E(I)-E(M))/(E(J)-E(M))+C1(M)
    8 CONTINUE
      DO15 I=3,L
      J=I
      IF(E(I).LT.-V)GO TO 18
      IF(C2(I) .EQ.0.0) 17,18
   17 J=J+1
      IF(C2(J).EQ.0.0 .AND. J.NE.N) GO TO 17
      M=I-1
      C2(I)= (C2(J)-C2(M))*(E(I)-E(M))/(E(J)-E(M))+C2(M)
   18 CONTINU
      RETURN
      END
```

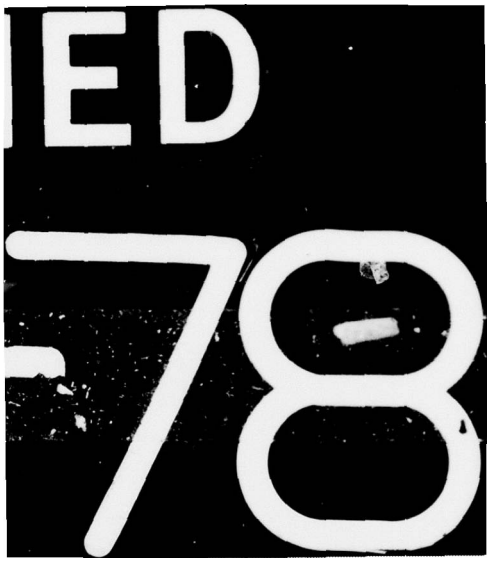
ED
78